The actin-based motor protein myosin II regulates MHC class II trafficking and BCR-driven antigen presentation

Fulvia Vascotto,[1] Danielle Lankar,[1] Gabrielle Faure-André,[1] Pablo Vargas,[1] Jheimmy Diaz,[1] Delphine Le Roux,[1] Maria-Isabel Yuseff,[1] Jean-Baptiste Sibarita,[2] Marianne Boes,[3] Graça Raposo,[2] Evelyne Mougneau,[4] Nicolas Glaichenhaus,[4] Christian Bonnerot,[1] Bénédicte Manoury,[1] and Ana-Maria Lennon-Duménil[1]

[1]Institut National de la Santé et de la Recherche Medicale Unité 653 and [2]Centre National de la Recherche Scientifique, Unité Mixte de Recherche 144 Institut Curie, 75005 Paris, France
[3]Department of Dermatology, Brigham and Women's Hospital, Harvard Medical School, Boston, MA 02115
[4]Institut National de la Santé et de la Recherche Medicale E0344, Université de Nice-Sophia Antipolis, Institut de Pharmacologie Moléculaire et Cellulaire, 06560 Valbonne, France

Antigen (Ag) capture and presentation onto major histocompatibility complex (MHC) class II molecules by B lymphocytes is mediated by their surface Ag receptor (B cell receptor [BCR]). Therefore, the transport of vesicles that carry MHC class II and BCR–Ag complexes must be coordinated for them to converge for processing. In this study, we identify the actin-associated motor protein myosin II as being essential for this process. Myosin II is activated upon BCR engagement and associates with MHC class II–invariant chain complexes. Myosin II inhibition or depletion compromises the convergence and concentration of MHC class II and BCR–Ag complexes into lysosomes devoted to Ag processing. Accordingly, the formation of MHC class II–peptides and subsequent CD4 T cell activation are impaired in cells lacking myosin II activity. Therefore, myosin II emerges as a key motor protein in BCR-driven Ag processing and presentation.

Introduction

Mature resting B lymphocytes capture antigen (Ag) via their specific B cell receptor (BCR), which corresponds to a surface Ig coupled to a signaling module formed by the Igα/Igβ dimer (Cambier et al., 1994; Reth and Wienands, 1997). In addition to Ag internalization, BCR stimulation triggers a complex cascade of signaling events that ultimately leads to the activation of B lymphocytes, which can then initiate the development of germinal centers. To complete germinal center formation, activated lymphocytes must process and present internalized Ag onto major histocompatibility complex (MHC) class II molecules to primed CD4 T cells, a process referred to as T-B cooperation (McHeyzer-Williams et al., 2000; Mitchison, 2004). It was recently shown that upon immunization, Ag-specific B lymphocytes are among the first lymphoid organ cells to acquire Ag and express the corresponding surface MHC–peptide complexes, highlighting the capacity of B cells to efficiently process and present BCR-internalized Ag onto MHC class II molecules in vivo (Byersdorfer et al., 2004; Catron et al., 2004).

MHC class II molecules assemble shortly after synthesis in the ER with a type II transmembrane protein, the invariant chain (Ii), which prevents their premature association with endogenous peptides (Wolf and Ploegh, 1995). In addition, Ii contains in its cytoplasmic tail the targeting signals that deliver MHC class II molecules into endocytic compartments for them to be loaded with antigenic peptides (Nakagawa and Rudensky, 1999; Villadangos et al., 1999; Watts, 2001). Such peptides result from the degradation of internalized Ag by endocytic proteases, which must also cleave Ii to free MHC II molecules for loading, a reaction catalyzed by the chaperone H2-DM (Nakagawa and Rudensky, 1999; Villadangos et al., 1999; Watts, 2001).

Therefore, successful Ag presentation relies on its efficient targeting into endocytic compartments competent for processing (i.e., wherein it concentrates together with MHC class II, proteases, and H2-DM molecules). This corresponds to an

Dr. Bonnerot died on 26 May 2004.

Correspondence to Ana-Maria Lennon-Duménil: ana-maria.lennon@curie.fr

Abbreviations used in this study: Ab, antibody; Ag, antigen; BCR, B cell receptor; DC, dendritic cell; LPS, lipopolysaccharide; MHC, major histocompatibility complex; MLC, myosin II light chain; NP, nanoparticle; OVA, ovalbumin.

The online version of this article contains supplemental material.

The Journal of Cell Biology, Vol. 176, No. 7, March 26, 2007 1007–1019
http://www.jcb.org/cgi/doi/10.1083/jcb.200611147

essential function of the BCR: Ag captured through the BCR undergoes accelerated transport to endosomes and enhanced presentation efficiency as compared with Ag taken up by fluid-phase endocytosis (Aluvihare et al., 1997; Cheng et al., 1999b). Translocation of BCR–Ag complexes to lipid rafts as well as an intact actin cytoskeleton have been proposed to be essential for accelerated transport to endosomes (Barois et al., 1998; Cheng et al., 1999a; Brown and Song, 2001). In addition, this process is accompanied by substantial modifications in the endocytic pathway of B cells, as highlighted by studies using various mouse lymphoma cell lines (Siemasko et al., 1998; Zimmermann et al., 1999; Lankar et al., 2002). In particular, we and others have shown that intracellular MHC class II molecules and BCR-internalized Ag converge into nonterminal LAMP-1–containing lysosomal compartments that display a multivesicular morphology and wherein Ag processing occurs, a process that depends on MHC class II–associated Ii (Siemasko et al., 1998; Zimmermann et al., 1999; Lankar et al., 2002).

The molecular mechanisms involved in the biogenesis of multivesicular endosomes have been documented, in particular by highlighting the importance of ubiquitylation in targeting membrane proteins to multivesicular endosome luminal vesicles (Raiborg et al., 2003). The key role of Ag-triggered BCR ubiquitylation in directing Ag trafficking toward multivesicular lysosomes enriched for MHC class II was recently reported (Drake et al., 2006). In addition, differential ubiquitylation of MHC class II β chain was shown to regulate its surface expression in immature versus mature dendritic cells (DCs; Shin et al., 2006). However, little information is available on the nature of the motor proteins that connect the vesicles carrying MHC class II molecules to the cytoskeleton, thereby helping their sorting to lysosome-like multivesicular compartments. This could involve microtubule- and/or actin-dependent forces, which are both known to control in concert the intracellular location and trafficking of organelles.

We aimed to understand how BCR engagement in primary lymphocytes coordinates the transport of Ag- and MHC

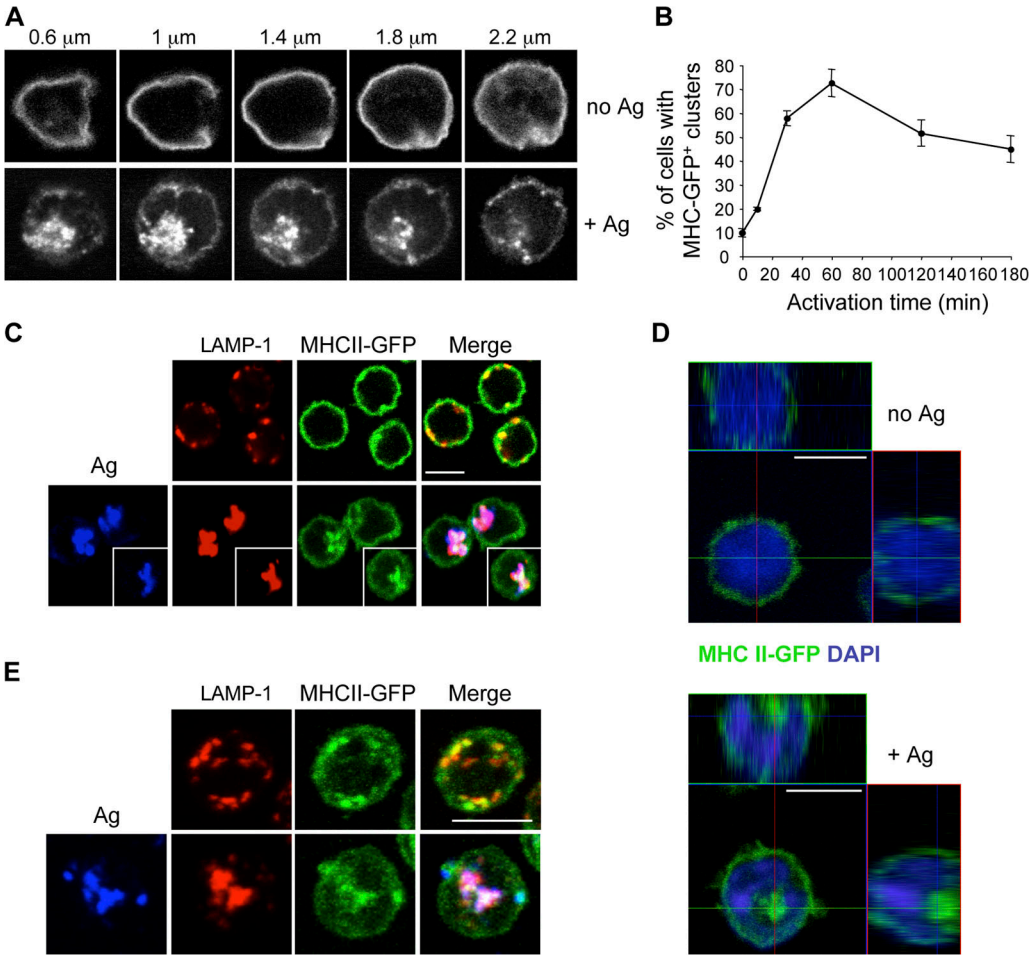

Figure 1. **BCR stimulation induces the convergence of BCR-internalized Ag and MHC II molecules in LAMP-1–containing vesicles that cluster toward the cell center.** (A and C–E) Confocal images of spleen B cells from MHC II–GFP mice. (A) Z sectioning of resting (top) or 1-h BCR-activated (bottom) cells. Resting cells display the peripheral distribution of MHC II–GFP molecules, whereas activated cells contain a central MHC II–GFP$^+$ cluster. (B) Clustering kinetics of MHC II–GFP-containing vesicles upon BCR engagement (n = 300 cells per time point; three independent experiments). Error bars represent SD. (C) MHC II–GFP$^+$ central clusters are LAMP-1$^+$ compartments wherein BCR-internalized Ag accumulates. The insets highlight cells coming from the same field but for which different z planes were used to build the final images. (D) Orthogonal projections of resting and BCR-stimulated MHC II–GFP$^+$ spleen B cells labeled with DAPI. Activated cells display a nuclear invagination where the central MHC II–GFP$^+$ lysosomal cluster sits. (E) 3D reconstructions of the single cells described in C. Bars, 5 μm.

class II–containing vesicles for them to converge and ensure efficient Ag processing. In this study, we identify the actin-based motor protein myosin II as playing an essential role in this process. Myosin II is activated upon BCR engagement and becomes physically associated with MHC class II–Ii complexes. Myosin II inhibition or depletion impairs the concentration of MHC class II molecules together with BCR–Ag complexes into lysosomes devoted to Ag processing. Accordingly, cells lacking myosin II activity do not efficiently form MHC class II–peptide complexes from BCR-internalized Ag. Thus, myosin II regulates MHC class II trafficking and Ag processing in B lymphocytes.

Results

BCR engagement induces clustering of MHC class II– and Ag-containing vesicles near the cell center

BCR stimulation of mouse B lymphoma cell lines triggers the appearance of MHC class II–containing compartments wherein BCR-internalized Ag is processed (Siemasko et al., 1998; Lankar et al., 2002). To explore the mechanisms underlying this process in primary B lymphocytes, we used MHC II–GFP knockin mice (Boes et al., 2002). B cells purified from the spleen of MHC II–GFP mice were or were not BCR stimulated with a polyvalent BCR ligand (hereafter referred to as Ag) and analyzed by confocal microscopy. Resting B cells exhibited the peripheral distribution of MHC II–GFP molecules (Fig. 1 A), which was reminiscent of both surface and intracellular localization (in both lysosomes and the ER; see the next paragraph; not depicted). In sharp contrast, BCR engagement induced the redistribution of MHC II–GFP-containing vesicles that clustered near the cell center (Fig. 1 A). A substantial change in the nuclear shape of BCR-activated lymphocytes was also observed: whereas the nucleus of resting cells was round and filled most of the intracellular space, the vast majority of stimulated B cells displayed an important nuclear invagination where the MHC-GFP$^+$ cluster sits (Fig. 1 D). Kinetics of MHC II–GFP clustering showed a peak at 60 min upon BCR triggering for ~70% of the cells (Fig. 1 B). A similar observation was recently made using MHC class II–GFP knockin mice expressing a specific BCR and stimulated with a polyvalent Ag (Kim et al., 2006).

MHC class II$^+$/Ag$^+$ clusters displayed the features of lysosomal-like Ag processing compartments: they stained positive for BCR–Ag complexes, LAMP-1, and H2-DM (Fig. 1, C and E; and Fig. S1 A, available at http://www.jcb.org/cgi/content/full/jcb.200611147/DC1) but contained reduced amounts of full-length Ii (Fig. S1 A). Accordingly, BCR stimulation induced the rapid cleavage of MHC II–bound Iip31 as indicated by the appearance of the Ii proteolytic intermediary fragments Iip25 and Iip10 (Fig. S1 B). No substantial change in the steady state levels of surface MHC class II was observed at any time period between 5 and 60 min upon BCR engagement (Fig. S1 C). Although this result does not exclude the possibility that MHC class II molecules are transported to lysosomes by trafficking through the cell surface, it indicates that the MHC class II$^+$/Ag$^+$ lysosomal cluster does not result from massive BCR-induced endocytosis of surface MHC class II molecules. Ultrastructural experiments showed that MHC class II$^+$/Ag$^+$ clusters corresponded to a network of vesicles and tubules, which included variable amounts of internal membranes enriched for MHC class II, LAMP-1, and H2-DM molecules (Fig. 2 and not depicted). No such compartment was observed in resting B cells (unpublished data). Therefore, we conclude that similar to mouse B lymphoma cells (Siemasko et al., 1998; Lankar et al., 2002), BCR-stimulated primary lymphocytes rapidly reorganize their endocytic route, accumulating lysosomal compartments that cluster near the center of the cell and to which MHC class II molecules and BCR–Ag complexes converge for processing.

Clustering of MHC II$^+$/Ag$^+$ lysosomes in BCR-stimulated cells is coupled to myosin II activation

We next used time-lapse video microscopy to analyze the dynamics of BCR-induced clustering of MHC class II–GFP$^+$ vesicles. Purified spleen MHC II–GFP$^+$ B cells were or were not

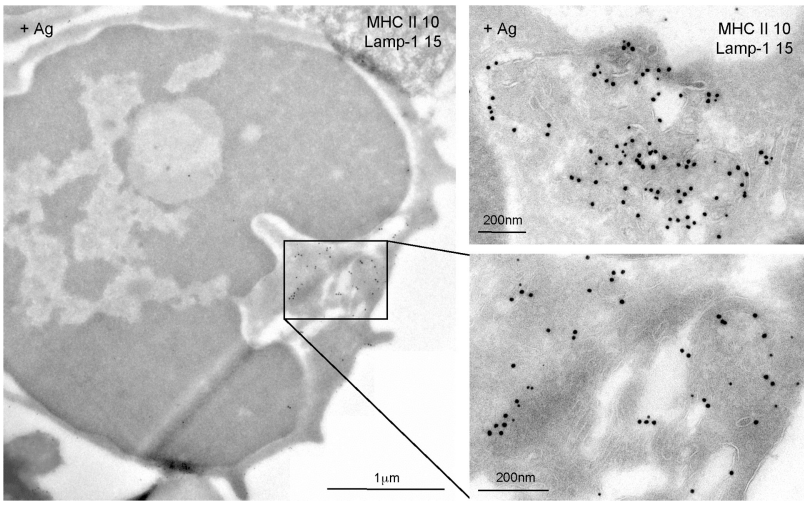

Figure 2. **Immunogold cryoelectron microscopy analysis of 1-h BCR-stimulated MHC II–GFP$^+$ spleen B cells.** The central cluster containing MHC II–GFP molecules corresponds to a tubular and vesicular network of LAMP-1$^+$ lysosomes. Sections were labeled using 10-nm and 15-nm immunogold particles for MHC class II and LAMP-1 molecules, respectively. The boxed area is magnified in the right bottom panel.

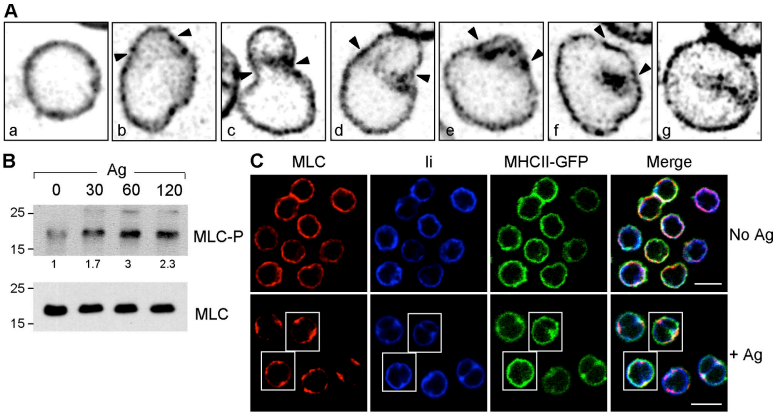

Figure 3. **Clustering of MHC II–containing lysosomes in activated B cells is coupled to cell contraction and myosin II activation.** (A) 2-h time-lapse analysis of purified MHC II–GFP$^+$ spleen B cells whose BCR was engaged when starting image collection. Deconvolved inverted grayscale z-stack projections of sequential images (a–g) from a single BCR-stimulated cell, which shows multiple membrane contraction events, are displayed (Video 3, available at http://www.jcb.org/cgi/content/full/jcb.200611147/DC1). Arrowheads indicate contracted membrane portions. (B) Cell lysates from B cells activated for different time periods with BCR polyvalent ligands were analyzed by immunoblotting using antiphospho-MLC (top) and anti-MLC Abs (bottom). Levels of phospho-MLC were quantified with ImageJ software (National Institutes of Health) and normalized for the relative intensity of total MLC. (C) Confocal images of fixed MHC II–GFP$^+$ spleen B cells labeled with anti-MLC and anti-Ii (In-1) Abs. Although resting B cells show the homogeneous cytoplasmic distribution of MLC, 30 min–stimulated cells redistribute their MLC molecules to contracted cell poles, where they colocalize with MHC II–GFP and Ii. The boxes highlight cells coming from the same slide but from a different field. Bars, 5 μm.

BCR stimulated and analyzed by 3D deconvolution time-lapse fluorescence microscopy. MHC II–GFP$^+$ vesicles showed random movements in resting B cells and did not experience any substantial change in morphology during the duration of image acquisition (Video 2; available at http://www.jcb.org/cgi/content/full/jcb.200611147/DC1). In contrast, Ag-activated B lymphocytes exhibited major morphological changes during time-lapse (see Video 1 for general field and Video 3 for single cell). Strikingly, the plasma membrane of the vast majority of B cells underwent successive contraction events after BCR engagement (Fig. 3 A and Videos 1 and 3). We consistently observed that cell contraction was coupled to MHC II–GFP clustering: MHC II–GFP clusters transiently associated with a contracted membrane portion and then moved toward the center of the cell (Fig. 3 A, arrowheads). Importantly, the centripetal movement of MHC II–GFP clusters occurred concomitantly to contraction arrest followed by cell spreading (Fig. 3 A and Video 3). We conclude that the dynamics of MHC class II–containing vesicle clustering are coupled to BCR-induced cell contractility.

Cell contractility is controlled by the actomyosin network and relies, in part, on phosphorylation of the regulatory myosin II light chain (MLC). MLC phosphorylation allows the activation of myosin II, which then initiates contraction by moving on actin microfilaments (Bresnick, 1999). To investigate whether myosin II was activated upon Ag stimulation, we analyzed the levels of phosphorylated MLC in resting and activated spleen B lymphocytes. Immunoblot experiments performed with an antibody (Ab) that specifically recognizes phosphorylated MLC showed that BCR stimulation considerably increased MLC phosphorylation (Fig. 3 B). MLC phosphorylation showed kinetics that was consistent with its potential implication in the BCR-induced clustering of MHC class II$^+$ vesicles, reaching maximal levels at 60 min upon BCR engagement (threefold as compared with nonactivated B cells).

Analysis of the subcellular distribution of MLC showed that although resting cells exhibited homogenous peripheral MLC distribution, a 30-min BCR stimulation induced the concentration of MLC in contracted cell portions, as contractile

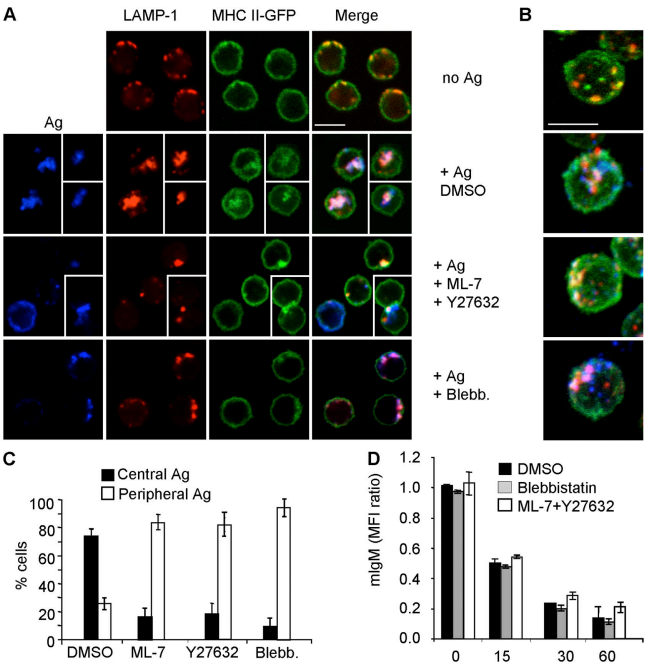

Figure 4. **Myosin II activation is required for the formation of lysosomal clusters where MHC class II and Ag converge but is not required for BCR capping and internalization.** (A) Confocal images obtained from MHC II–GFP$^+$ spleen B cells not pretreated or pretreated with 10 μM ML-7 plus 10 μM Y27632 or 70 μM blebbistatin and activated with multivalent BCR ligands for 1 h at 37°C. Fixed cells were labeled with the indicated Abs. ML-7/Y27632 or blebbistatin treatment prevents the central clustering of MHC II–GFP$^+$/LAMP-1$^+$/Ag$^+$ vesicles. Insets show cells coming from the same slide but from different fields. (B) 3D reconstructions of the single cells described in A. (C) Quantification of the experiment described in A (n = 200; three independent experiments). Histogram bars represent the percentage of activated B cells that show central (black) or peripheral (white) MHC II–GFP$^+$/Ag$^+$ vesicles. (D) BCR internalization kinetics in spleen B cells not treated or treated with ML-7/Y27632 or blebbistatin and stimulated with BCR polyvalent ligands. The levels of plasma membrane IgM (mIgM) were assessed by cytofluorometry on B220$^+$ gated cells. Histogram bars represent mean fluorescence intensity ratios between BCR-activated and resting B cells from three different experiments. Error bars represent SD. Bars, 5 μm.

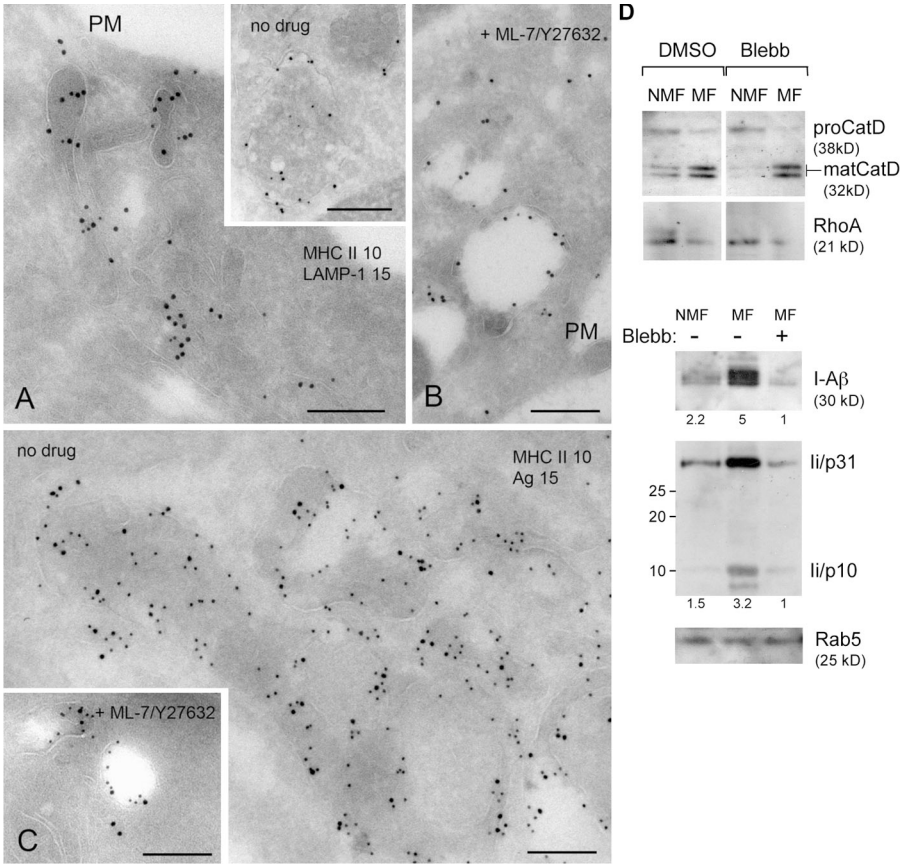

Figure 5. **Myosin II activation is required to concentrate Ag and MHC II molecules into clustered lysosomes.** (A–C) Cryoimmunoelectron microscopy analysis of 1 h–activated spleen B cells pretreated with DMSO (A and C) or ML-7 plus Y27632 (10 μM of each; B and C, inset) and labeled for MHC II (10 nm gold particles) and LAMP-1 molecules (A and B) or Ag (C). Activated cells display a network formed of LAMP-1$^+$ tubular and vesicular lysosomes wherein the Ag and MHC class II molecules concentrate together (A and C). Myosin II–inhibited cells show vacuolar compartments that label for Ag, MHC II, and LAMP-1 at their limiting membrane (B and C, inset). PM, plasma membrane. Bars, 200 nm. (D) Immunoblotting of the nonmagnetic (NMF) and magnetic fractions (MF) obtained from spleen B cells not pretreated or pretreated with blebbistatin, stimulated with magnetic NP coupled to F(ab')$_2$ anti-BCR Abs, and mechanically lysed. Semipurified Ag-containing endosomes were obtained after magnetic separation as described in Materials and methods. Enrichment for MHC class II and Ii in the magnetic fraction is decreased in blebbistatin-treated cells. The levels of cathepsin D (proform and mature) and Rab5 in the magnetic fraction are not affected by blebbistatin treatment.

rings were often appreciated (Fig. 3 C). Both MHC II–GFP and Ii were enriched in such contraction sites together with MLC molecules (Fig. 3 C, bottom). This finding strengthens the time-lapse results showing that before moving toward the center of the cell, clusters of MHC class II$^+$ vesicles transiently associate with contractile membrane portions. Thus, BCR stimulation of resting mature lymphocytes triggers myosin II activation as indicated by MLC phosphorylation and redistribution to contracted membrane portions, where it colocalizes with MHC class II$^+$ vesicle clusters.

Myosin II activity is required for the clustering and maturation of lysosomes wherein MHC class II molecules and BCR–Ag complexes concentrate

To demonstrate that myosin II–driven contraction is indeed functionally required for BCR-induced clustering of MHC class II– and Ag-containing vesicles, we first used pharmacological inhibitors. The inhibitors Y27632 and ML-7 target RhoA effector kinase (Rho-associated kinase) and MLC kinase, respectively (Kimura et al., 1996). Rho-associated kinase inhibits MLC-phosphatase and, thereby, indirectly promotes the levels of phosphorylated MLC, a task performed by MLC kinase (Kimura et al., 1996). Blebbistatin is a highly specific inhibitor of the ATPase activity of myosin II that has been used to demonstrate its involvement in cell division and migration (Straight et al., 2003; Rosenblatt et al., 2004; Gomes et al., 2005; Gupton and Waterman-Storer, 2006). Time-lapse experiments showed that when spleen B cells were pretreated for 45 min with these inhibitors before Ag stimulation, they underwent neither contraction nor cell spreading (Videos 4 and 5, available at http://www.jcb.org/cgi/content/full/jcb.200611147/DC1).

Prevention of myosin II activation or inhibition of its activity strongly impaired the clustering of MHC class II– and Ag-containing lysosomes at the center of BCR-stimulated spleen B cells (Fig. 4, A and B). Only a few clusters were observed in drug-treated activated cells, and they seemed to contain reduced amounts of MHC class II, LAMP-1, and Ag molecules. In addition, these clusters remained dispersed at the cell periphery rather than concentrated at the center of myosin II–inhibited cells (Fig. 4, A and B). Quantitative analysis showed that although ~75% of control Ag-stimulated cells displayed MHC II–GFP$^+$/LAMP-1$^+$/Ag$^+$ central clusters, only ~15% did when myosin II activation was hampered (n = 200; Fig. 4 C). Impaired clustering did not result from a defect in Ag-induced BCR capping or internalization, which remained unaffected in the presence of myosin II inhibitors, excluding a general paralysis induced by drug treatment (Fig. 4 D and Fig. S2, available at http://www.jcb.org/cgi/content/full/jcb.200611147/DC1). No effect of myosin II inhibition on MHC class II surface levels was observed by cytofluorometry (unpublished data). Thus, MHC class II– and Ag-containing vesicles do not converge and cluster together at the cell center when myosin II activity is compromised.

Having shown that myosin II activity is required for the proper positioning of MHC II$^+$/Ag$^+$ compartments, we next

Table I. **Inhibition of myosin II activity reduces the amount of Ag and MHC class II molecules that concentrate together in lysosomes**

	Ag	MHC II	Ratio of Ag/MHC II
DMSO-treated cells	200	663	0.302
ML-7/Y27632-treated cells	28	288	0.123

Quantification of the immunogold cryoelectron microscopy experiments shown in Fig. 5. Gold particles from 30 compartments were counted in randomly selected B cell profiles. We could estimate that the compartments presenting vacuolar empty morphology in drug-treated cells represent ~70% of the total compartments observed. No vacuolar compartment was observed in non-treated cells.

addressed by immunogold cryoelectron microscopy whether it also affects the maturation of these vesicles. The network of tubular and vesicular lysosomes wherein LAMP-1, H2-DM, Ag, and MHC class II molecules accumulate was barely observed in cells lacking myosin II activity (Fig. 5, A and C). Instead, drug-treated BCR-stimulated lymphocytes showed vacuolar compartments that labeled for LAMP-1, Ag, or MHC class II molecules at their limiting membrane (Fig. 5, B and C; inset). Consistent with immunofluorescence experiments, these vacuolar compartments were dispersed in the cytoplasm of drug-treated cells rather than clustered together, leading to the reduced concentration of MHC class II molecules and Ag in their lumen as compared with control BCR-stimulated lymphocytes (see Table I for quantifications). Thus, the lack of myosin II activity affects the maturation of lysosomes to which MHC class II molecules and BCR–Ag complexes are targeted.

The impact of myosin II inhibition on the maturation of MHC II^+/Ag^+ lysosomes was further investigated by biochemical means using magnetic nanoparticles (NPs) coupled to anti-BCR Abs. As shown by Perrin-Cocon et al. (2004), these NPs undergo proper BCR-mediated uptake and targeting to MHC class II–containing lysosomes (Fig. S3, available at http://www.jcb.org/cgi/content/full/jcb.200611147/DC1), allowing us to semi-purify the endocytic compartments in which they accumulate (Fig. 5 D). We found that both the amounts of MHC class II and Ii were strongly decreased in endosomes purified from BCR-stimulated cells whose myosin II activity was compromised (Fig. 5 D). In contrast, levels of the early endosomal marker Rab5 and of lysosomal mature cathepsin D found in the magnetic fraction were not affected by the lack of myosin II activity (Fig. 5 D). In conclusion, both our morphological and biochemical results indicate that myosin II is required for the proper trafficking and maturation of MHC class II– and Ag-containing vesicles: it promotes their clustering in activated B lymphocytes and, thereby, allows them to concentrate together into a multivesicular and tubular lysosomal network.

Myosin II activity is required for BCR-driven Ag presentation

We next assessed whether myosin II activity is required for the presentation of BCR-internalized Ag using both B lymphoma cells and primary B lymphocytes. A20/DNP cells were pretreated with Y27632 and/or ML-7, further incubated with ovalbumin (OVA)-DNP (DNP-OVA), fixed, and cultured together with OVA-responding T cell hybridoma (Peterson and Miller, 1990). Pretreatment of A20/DNP cells with drugs that prevented myosin II activation or activity inhibited OVA presentation to $CD4^+$ T cells in a dose-dependent manner (Fig. 6, A, B, and D). Equivalent results were obtained when targeting OVA protein to the BCR of spleen B cells by chemically cross-linking it to anti-IgM F(ab′) fragments (Fig. 6 C). No presentation of non-coupled OVA was detected under such experimental conditions, showing that the effect of the drugs indeed concerned the presentation of BCR-internalized Ag (Fig. 6 C). Importantly, the presentation of exogenously added $OVA_{323–339}$ peptide was not affected by any drug treatment, demonstrating that the inhibition of Ag presentation resulted from impaired processing (Fig. 6, A, C, and D). Pulse-chase experiments performed on Ag-stimulated spleen B cells not treated or treated with the drugs showed that synthesis, maturation, and processing of MHC II molecules were not compromised upon myosin II inhibition: equivalent amounts of SDS αβ–peptide complexes were immunoprecipitated from control and drug-treated cells. This indicates that the basal interaction of neosynthesized MHC II molecules with endogenous peptides does not require

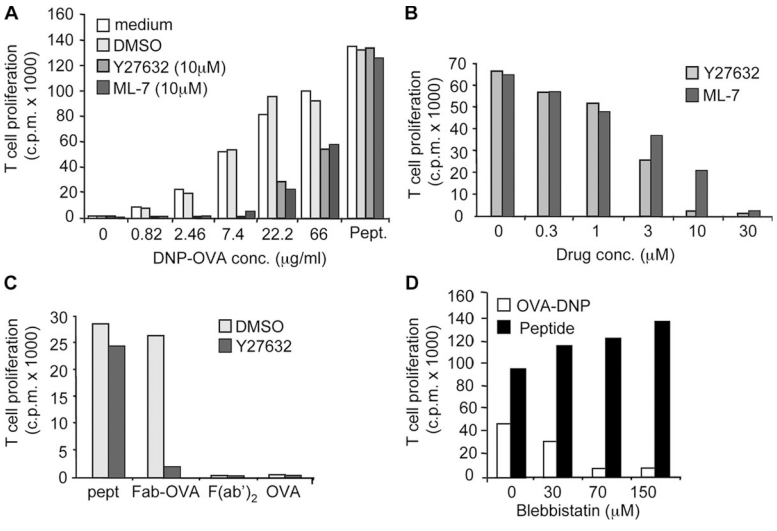

Figure 6. **Myosin II activity is required for BCR-driven Ag presentation.** (A and B) A20 cells expressing an anti-DNP surface IgM were pretreated with ML-7, Y27632, or DMSO for 45 min, incubated with DNP-OVA (increasing amounts [A] or 10 μg/ml [B]) or 20 μg/ml $OVA_{323–339}$ peptide for 4 h, washed, and fixed. T cell activation was measured as described in Materials and methods. T cell proliferation in response to DNP-OVA presentation is inhibited by the inhibitor treatment in a dose-dependent manner. (C) Spleen B cells pretreated with Y27632 or DMSO for 45 min at 37°C were incubated with anti-IgM F(ab′) chemically cross-linked to OVA, noncoupled OVA, anti-IgM $F(ab')_2$, or with OVA peptide for 4 h and were washed and fixed. (D) The experiment was performed as in A but not pretreating or pretreating the cells with blebbistatin.

myosin II activity, whereas the processing of BCR-internalized Ag strictly relies on it (Fig. S4, available at http://www.jcb.org/cgi/content/full/jcb.200611147/DC1). Thus, the activity of the actin-associated motor myosin II is strictly required for BCR-driven Ag presentation.

Myosin II is required for the formation of MHC II–peptide complexes from BCR-uptaken Ag

Is myosin II necessary for the formation of MHC II–peptide complexes from BCR-uptaken Ag, or is it required to export these complexes to the cell surface for interaction with T cells? To address this question, we took advantage of the mAb 2C44 that specifically recognizes the complexes formed between I-A^d molecules and the 156–173 peptide from *Leishmania major* Ag LACK but does not bind to any of the free components (Lazarski et al., 2006). Recombinant LACK protein was targeted to BCR uptake by coupling it to the aforementioned NP together with anti-BCR Abs. The appearance of I-A^d–$LACK_{156–173}$ complexes was analyzed by immunofluorescence using 2C44 at 2 and 4 h upon Ag internalization. At both time points, I-A^d–$LACK_{156–173}$ complexes were mainly detected in lysosome clusters that labeled for LAMP-1 (Fig. 7 A). No complex formation was observed when using NPs only coupled to LACK or to anti-BCR Abs (Fig. 7 B and not depicted).

This assay was used to assess the requirement of myosin II activity on the formation of MHC II–peptide complexes. Blebbistatin treatment strongly reduced the percentage of $2C44^+$ cells, indicating that myosin II activity is indeed necessary for the formation of I-A^d–$LACK_{156–173}$ complexes (see Fig. 7, A and B for quantifications). Moreover, the few $2C44^+$ blebbistatin-treated cells displayed staining in peripherally distributed lysosomes rather than in central clusters (Fig. 7 A). Impairment of I-A^d–$LACK_{156–173}$ complex formation in myosin II–inhibited cells was further confirmed biochemically by showing that they contained reduced 2C44-reactive material after immunoprecipitation as compared with mock-treated lymphocytes (Fig. 7 C).

To introduce genetic evidence in the involvement of myosin II in the formation of MHC II–peptide complexes, we performed depletion experiments using siRNA. RT-PCR analysis had shown that MyH9 was a major myosin II form expressed in mouse B lymphoma cells (unpublished data). Three myosin IIA

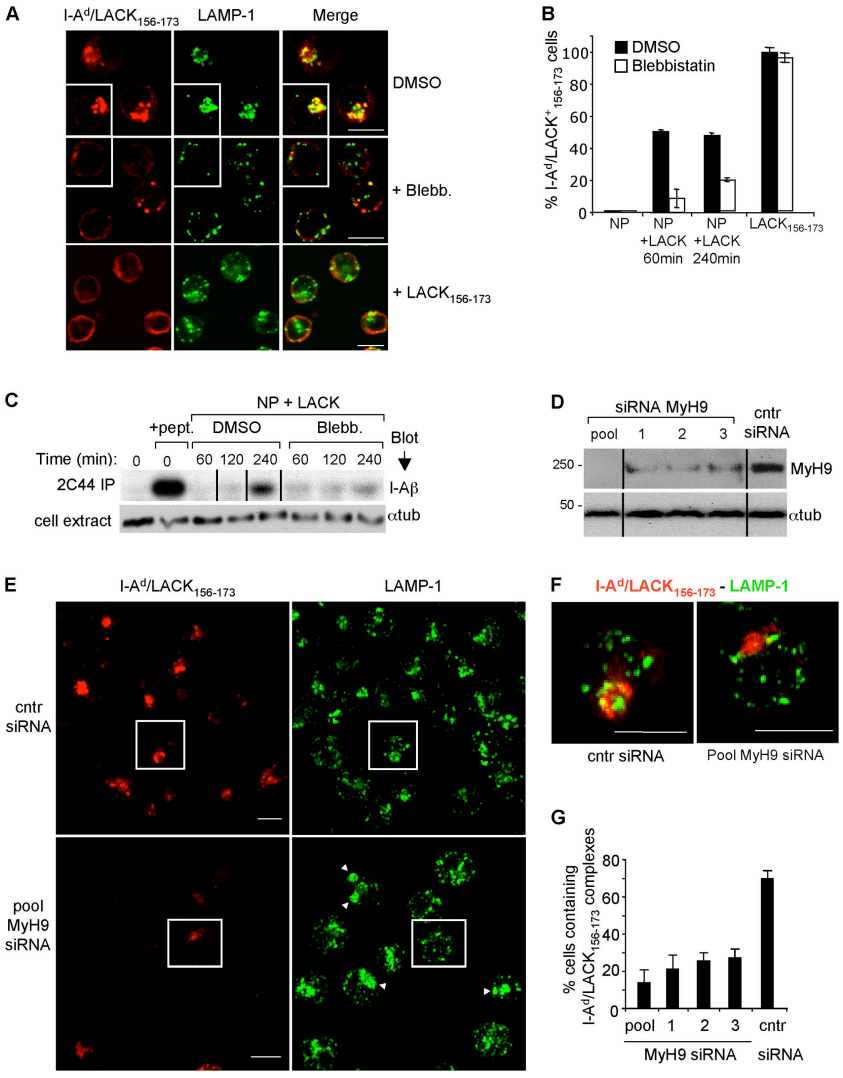

Figure 7. **Myosin II is required for the formation of MHC II–peptide complexes.** (A–C) Blebbistatin inhibits the formation of I-A^d–$LACK_{156–173}$ complexes. (A) Confocal images of IIA1.6 cells not pretreated or pretreated with 70 μM blebbistatin and activated for 4 h at 37°C with NP coupled to recombinant LACK protein and $F(ab')_2$ anti-BCR Abs in a 1:1 molarity ratio. Cells were fixed and labeled with the indicated Abs. Peptide $LACK_{156–173}$ was used as a positive control for 2C44 staining (bottom). Insets show cells coming from the same slide but from different fields. (B) Quantification of the experiment described in A (n = 300; three independent experiments). Histogram bars represent the percentage of activated B cells that contain I-A^d–$LACK_{156–173}$ complexes. NPs were coupled to anti-BCR $F(ab')_2$ Abs alone (NP) or together with recombinant LACK protein. Error bars represent SD. (C) IIA1.6 cells not pretreated or pretreated with blebbistatin were activated as described in A. Peptide $LACK_{156–173}$ was added to the cells for 4 h at 37°C as a positive control. Cells were lysed, immunoprecipitated with 2C44, and analyzed by immunoblotting for the presence of I-Aβ. In parallel, equal amounts of cell extracts were analyzed by immunoblotting for α-tubulin expression. Vertical lines indicate gel image cuts. (D–F) Myosin II depletion by siRNA impairs lysosome clustering and formation of I-A^d–$LACK_{156–173}$ complexes. (D) IIA1.6 cells were transfected with different siRNAs specific for myosin IIA (*MyH9* gene; pool of three single siRNAs) or with a control siRNA and incubated at 37°C for 96 h. Cells were lysed, and equal amounts of cell lysates were analyzed by immunoblotting for the presence of myosin II heavy chain. α-Tubulin was used as a loading control. (E) Confocal images of IIA1.6 cells transfected for 96 h with control or the pool of MyH9 siRNAs, activated for 4 h, fixed, and stained as described in A. Arrowheads indicate peripheral lysosome patches in MyH9-depleted cells. The boxed areas are magnified in F. (F) Magnified images of the single cells shown in E. (G) Quantification of the experiments described in E (n = 300; two independent experiments). Histogram bars represent the percentage of activated B cells that contain I-A^d–$LACK_{156–173}$ complexes. Error bars represent SD. Bars, 5 μm.

(MyH9)–specific siRNAs were electroporated into B lymphocytes either individually or as a pool. MyH9 depletion was obtained with the three individual siRNAs and even more efficiently when using the siRNA pool (Fig. 7 D). The percentage of $2C44^+$ cells was considerably reduced by MyH9 depletion (see Fig. 7, E–G for quantifications), demonstrating that the absence of myosin II severely compromised the formation of $I\text{-}A^d$–$LACK_{156–173}$ complexes from BCR-internalized LACK. As expected, MyH9 depletion reduced the frequency of central lysosome clusters (Fig. 7, E and F). In addition, certain MyH9-depleted cells exhibited peripheral LAMP-1^+ patches similar to the ones observed in stimulated primary B cells whose myosin II activity was compromised (Fig. 7 E, arrowheads). Therefore, we conclude that myosin II is essential for the efficient formation of MHC II–peptide complexes from BCR-internalized Ag.

MHC II–Ii complexes and myosin II dynamically associate upon BCR engagement

Having established that myosin II activity regulates the trafficking of MHC class II molecules upon BCR engagement, we next investigated whether these proteins physically associate. The trafficking of MHC class II molecules mainly relies on the cytosolic portion of its chaperone-associated molecule, Ii, which is essential for the processing and presentation of BCR-internalized Ag (Zimmermann et al., 1999). Thus, we raised the hypothesis that Ii may physically link MHC class II–containing vesicles to myosin II through its cytosolic tail. In support of this hypothesis, B cells stimulated for short time periods showed a strong Ii staining in the contracted membrane portions and the contractile rings to which MLC and MHC class II molecules were recruited (Fig. 3 C) as well as Ii/MLC colabeling in membranes from ER, Golgi, and endocytic vesicles when analyzed by immunogold cryoelectron microscopy (Fig. S5, available at http://www.jcb.org/cgi/content/full/jcb.200611147/DC1).

Moreover, MLC was pulled down in the aforementioned B lymphoma cell line by using anti-Ii Abs in coimmunoprecipitation experiments (Fig. 8 A). MHC class II molecules were also found in anti-Ii immunoprecipitates. Strikingly, MLC–Ii complexes were retrieved from BCR-stimulated cells only. The interaction was found to be transient, and its kinetics was compatible with the one observed for MHC II^+ vesicle clustering, reaching maximal levels at 60 min and then decaying. In agreement with this observation, the amounts of Ii-associated actin increased with similar kinetics as well (Fig. 8 A). MLC was also retrieved when using anti-MHC II Abs for the immunoprecipitation (Fig. 8 B). Importantly, the inhibition of myosin II activity with blebbistatin reduced its ability to associate with MHC class II–Ii complexes (Fig. 8 B). These results show that MHC II–Ii complexes and myosin II dynamically associate upon BCR engagement and further indicate that BCR-triggered myosin II activity is necessary for this association.

Association of MHC class II to myosin II requires Ii

Are both Ii and MHC class II required for the association to myosin II? Because insufficient protein amounts are generated from mouse spleen B cells, we used DCs purified from either Ii- or MHC II (I-Aβ)–deficient mice to address this question. Indeed, a 30-min lipopolysaccharide (LPS) stimulation of DCs induces the dynamic association between MHC class II–Ii and myosin II, as observed in BCR-activated cells (unpublished data). We found that the interaction between MHC class II and MLC was completely abolished in Ii-deficient cells (Fig. 9 A). This equally applies to myosin II heavy chain (MyH9) as observed when immunoprecipitating Ii and analyzing the coimmunoprecipitated material by immunoblotting or by an unbiased detection method (Coomassie staining followed by mass spectrometry analysis). Indeed, MyH9 is the major protein retrieved in this experiment, and its levels are comparable with those of immunoprecipitated Ii (Fig. 9 C). Strikingly, Ii retained the capacity to associate to MLC in I-Aβ knockout cells, although less efficiently (Fig. 9 A). No difference in the expression levels of MLC or myosin II heavy chain was observed in total extracts from I-Aβ– or Ii-deficient cells (Fig. 9 B). Together, these results show that Ii is essential for MHC II–Ii–myosin II interaction and further suggests that this association links MHC class II–containing vesicles to the actin network. In support of this conclusion, we found that Ii-deficient BCR-stimulated lymphocytes exhibited the peripheral distribution of MHC II–, LAMP-1–, and Ag-containing vesicles instead of central clusters, which is similar to cells whose myosin II activity was compromised (Fig. 9 E).

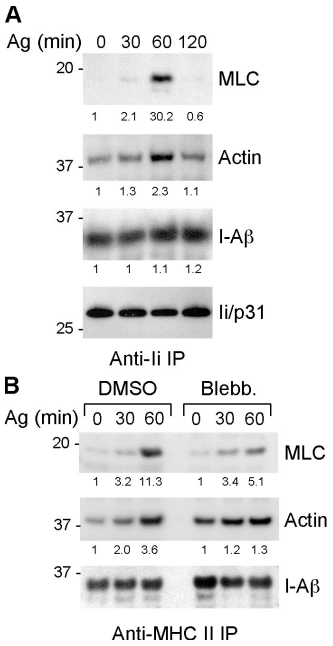

Figure 8. **MHC class II–Ii complexes and myosin II transiently associate upon BCR engagement.** (A and B) Coimmunoprecipitation experiments showing dynamic MHC class II–Ii–MLC association upon BCR engagement. IIA1.6 cells were activated with multivalent BCR ligands and lysed in a 0.5% NP-40–containing buffer, and immunoprecipitations were performed using anti-Ii (In-1; A) or anti–MHC II Abs (M5114; B). Immunoprecipitates were analyzed by immunoblotting for the presence of MLC, actin, Ii, or MHC II (I-Aβ). Myosin II inhibition by 70 μM blebbistatin reduces MHC II–Ii–myosin II association (B). Quantifications were performed with ImageJ software, and values were normalized to the immunoprecipitated protein levels and expressed relative to the signal intensity obtained from nonstimulated cells.

Two nonexclusive hypotheses can be raised to explain the lack of MHC II–myosin II association in Ii-deficient cells: it could result from (1) MHC II mislocalization, which accumulates in the ER when Ii is missing (Koonce and Bikoff, 2004; unpublished data), or (2) the requirement for Ii cytosolic tail to form a complex with myosin II. The fact that Ii retains its ability to associate to myosin II in the absence of MHC class II molecules argues in favor of the second hypothesis. To further analyze the involvement of Ii cytosolic tail in the association with myosin II, we took advantage of the specific inhibitor of cathepsin S, LHVS, which prevents the removal of Ii cytosolic tail from MHC II–Ii complexes that have reached LAMP-1$^+$ compartments (Brachet et al., 1997; Driessen et al., 1999). LHVS-treated cells displayed modified kinetics of MHC II–myosin II association: although 60 min upon BCR activation, the retrieval of myosin II with anti–MHC II Abs was diminished as compared with untreated cells, the association was still maintained 120 min upon BCR engagement (Fig. 9 D). This result shows that the presence of the cytosolic tail of Ii on MHC II–Ii complexes in lysosomes regulates their ability to associate with myosin II. We conclude that the lack of association of MHC II to MLC in Ii- deficient cells likely reflects the direct involvement of Ii in the formation of this protein complex rather than from the mislocalization of MHC class II molecules. Our data further indicate that MHC II–Ii–myosin II association can be modified by inhibiting myosin II activity with blebbistatin as well as by altering the processing of MHC II–Ii complexes with LHVS, providing strong evidence in favor of a direct role for myosin II in regulating MHC class II trafficking.

Discussion

In this study, we show that BCR engagement deeply modifies the endocytic pathway of B cells by inducing the formation of lysosome clusters wherein MHC class II molecules and BCR–Ag complexes converge. This process relies on the motor protein myosin II. We propose that BCR engagement triggers myosin II activation and association with MHC class II–Ii complexes, allowing them to be transported toward incoming BCR-associated Ag. This event of polarized trafficking would allow MHC class II and BCR–Ag complexes to concentrate together in lysosomal compartments devoted to Ag processing that cluster near the cell center. The association between MHC class II–Ii complexes and myosin II is likely to be mediated by Ii cytosolic tail and, thus, is likely to be favored by the previously reported BCR-triggered down-regulation of cathepsin S activity, which allows the transient accumulation of MHC II–Ii complexes that retain Ii cytosolic tail (Lankar et al., 2002). Once in lysosome clusters, the proteolysis of Ii, which, as shown in Fig. S1, is triggered upon BCR engagement, would help myosin II to dissociate from MHC class II–containing vesicles. Accordingly, inhibition of myosin II activity prevents the concentration of MHC class II and Ag–BCR complexes in clustered lysosomes as well as the subsequent formation of MHC class II–peptide complexes and presentation to T cells. Therefore, myosin II emerges as the first motor protein to be involved in Ag-regulated trafficking of MHC class II molecules.

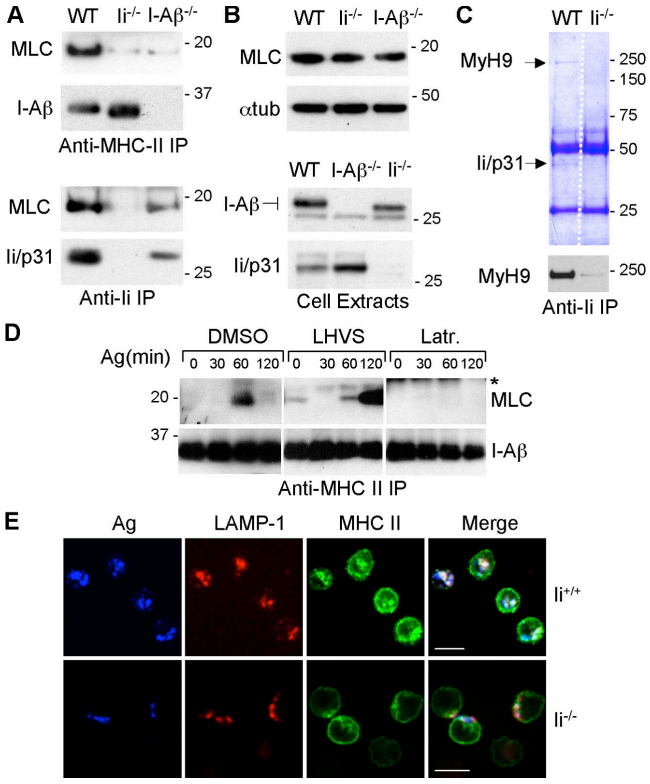

Figure 9. **Ii is required for MHC II–myosin II association.** (A–D) Coimmunoprecipitation experiments highlighting the key role of Ii in MHC II–MLC association. (A) Bone marrow–derived DCs from wild-type (WT), Ii-, or I-Aβ–deficient mice were treated with LPS for 30 min and lysed in a 0.5% NP-40–containing buffer, and immunoprecipitations were performed as described in Fig. 7. (B) Immunoblotting analysis of extracts from bone marrow–derived DCs from wild-type, Ii-, or I-Aβ–deficient mice. Cell were treated with LPS for 30 min and lysed in a 0.5% NP-40–containing buffer. 10 μg of protein was loaded per lane. I-Aβ glycosilation is impaired in Ii-deficient cells, and total levels of Ii are increased in extracts from DCs lacking I-Aβ. (C) Coomassie blue–stained gel (top) and immunoblotting experiment (bottom) showing the association of Ii with myosin II heavy chain. Bone marrow–derived DCs from wild-type or Ii-deficient mice were treated as described in A, and anti-Ii immunoprecipitations were performed using the In-1 Ab. Dotted line indicates a gel image cut. (D) Modification of the presence of MHC II–associated Ii cytosolic tail by LHVS treatment alters the kinetics of MHC II–myosin II interaction. IIA1.6 cells were not pretreated or pretreated with 5 nM LHVS or latrunculin B, activated with multivalent BCR ligands, and lysed in a 0.5% NP-40–containing buffer, and immunoprecipitations were performed using anti–MHC II Abs (M5114). The top band shown with an asterisk in latrunculin-treated samples corresponds to the light chain of the membrane Ig, which is further solubilized during lysis when the actin cytoskeleton is disrupted. (E) Confocal images obtained from spleen purified B cells of Ii$^{+/+}$ and Ii$^{-/-}$ mice activated with multivalent BCR ligands for 1 h that were fixed and stained with the indicated Abs. The lack of Ii molecules prevents the clustering of MHC II$^+$/Ag$^+$ lysosomes toward the cell center similarly to myosin II inhibition. Bars, 5 μm.

Is myosin II–driven cell contraction required for BCR-driven Ag processing?

Myosin II is known to mediate cellular contractility. Our video microscopy experiments show that BCR-stimulated lymphocytes display major contractile activity, which is suppressed when inhibiting myosin II activation. Does cell contraction mediate the clustering of MHC II–containing lysosomes? Although we cannot directly address this question, we do favor this hypothesis based on the following observations: (1) the clusters of

MHC class II–GFP$^+$ vesicles were consistently found in association with contracted membrane portions during live imaging; (2) the regulatory subunit of myosin II was relocalized together with MHC II–Ii complexes to these contracted areas in experiments on fixed cells; and (3) the kinetics of MHC II–Ii–myosin II interaction was compatible with the one followed by cell contraction.

An attractive hypothesis would be to propose that actomyosin contractility would create the forces required for B cells to extract Ag from target cell membranes (Batista et al., 2001). Indeed, it is thought that in vivo, B lymphocytes mainly acquire Ag in a membrane-bound form from cells in charge of transporting them from the periphery to the lymph nodes (Qi et al., 2006). The acquisition of membrane-bound Ag by B cells is dependent on the interaction of the ICAM-1/LFA-1 adhesion molecules (Carrasco et al., 2004), which were shown to trigger actomyosin contraction in other cell types (Smith et al., 2003). Interestingly, we often observed contacts between Ag-stimulated B cells undergoing contractions during our time-lapse experiments (Video 1). Therefore, ICAM-1/LFA-1 might potentiate the activation of myosin II at the contact site between B and Ag carrier cells and, thereby, couple BCR-triggered activation to Ag extraction (Carrasco et al., 2004). Accordingly, it was recently demonstrated that extraction of membrane-bound Ag by B lymphocytes occurs through a two-phase membrane spreading and contraction response (Fleire et al., 2006), which is likely to depend on the actomyosin network.

MHC II–Ii–myosin II interaction links MHC II trafficking to the actomyosin network

The molecular link between MHC class II–containing compartments and the actomyosin network is provided by the dynamic interaction between MHC class II–Ii complexes and myosin II, which become part of a protein complex that specifically assembles upon BCR engagement and requires myosin II activation as well as proper processing and trafficking of MHC II–Ii complexes. The specificity of this protein interaction was confirmed by showing that it relies on the strength of BCR signaling given that it is substantially impaired in Syk-deficient cells (unpublished data). In addition, myosin IIA heavy and light chains were recently identified in a unbiased proteomic approach as coimmunoprecipitating with MHC class II molecules in human DCs, further strengthening the relevance of the MHC II–myosin II association reported in this study by showing that it is conserved in human DCs (Benaroch, P., personal communication).

Although we have much evidence suggesting that the physical association between MHC class II molecules and myosin II involves the cytosolic tail of Ii, we do not know whether this is a direct protein interaction. Interestingly, a comparative analysis of the lipid raft proteomics identified both myosin IIA heavy and light chains as becoming associated with lipid rafts upon BCR engagement (Gupta et al., 2006). Association to membrane microdomains such as lipid rafts has been highlighted for both BCR–Ag and MHC class II–Ii complexes (Pierce, 2002; Poloso et al., 2004). In addition, a positive correlation between membrane microdomain association, productive trafficking toward the center of the cell, and Ag presentation by MHC class II molecules was recently shown for oligomeric BCR ligands (as opposed to monomeric ones; Kim et al., 2006). Thus, MHC II–Ii and myosin II might be part of a complex of proteins that dynamically forms and associates with membrane microdomains upon BCR activation. Because actin dynamics were shown to control the BCR-induced reorganization of lipid rafts (Hao and August, 2005), it is tempting to propose that myosin II could play a direct role in recruiting proteins such as MHC class II–Ii complexes to these microdomains. As demonstrated here for myosin II activity, association to lipid rafts was indeed suggested to be required for the formation of MHC class II–peptide complexes (Pierce, 2002; Poloso et al., 2004).

How does myosin II direct the trafficking of MHC class II–carrying vesicles?

Myosin II could directly transport MHC class II–Ii-containing vesicles along actin microfilaments, thereby directing their movement toward the incoming vesicles that carry BCR–Ag complexes. Indeed, although myosin II was described as a nonprocessive motor protein (i.e., it spends only a small part of its ATP hydrolysis cycle bound to actin cables and is therefore thought to be unable to transport cargoes on long distances; Frank et al., 2004), oligomerized myosin II molecules might be able to mediate cargo transport. Alternatively, myosin II could act indirectly, possibly by helping to connect the transport of MHC II–containing vesicles, which were shown to use microtubules to travel into cells (Wubbolts et al., 1999), to the trafficking of Ag-carrying vesicles, which are most likely associated with the actin cortex (Barois et al., 1998; Brown and Song, 2001). Accordingly, myosin II was shown to coordinate the interactions between actin filaments and microtubules and might thereby affect the transport of associated organelles (Frank et al., 2004; Seabra and Coudrier, 2004). In particular, changes in the polarization of the microtubule network during cell division and in migrating cells were attributed to myosin II activity (Rosenblatt et al., 2004; Gomes et al., 2005). Determining whether the role of myosin II in MHC class II trafficking in B lymphocytes is associated with the acquisition of a polarized phenotype as in their T counterpart (Jacobelli et al., 2004) requires further investigation.

In conclusion, we show here that B cells coordinately reorganize their actin cytoskeleton and endocytic pathway in response to an antigenic stimulus, an event that depends on the actin-based motor protein myosin II and is absolutely required for the processing of BCR-internalized Ag and presentation to CD4 T cells. This study provides the first evidence for the direct involvement of a motor protein in the regulation of MHC class II trafficking in Ag-presenting cells and further suggests the potential implication of myosin II in the trafficking of proteins that follow similar routes to MHC class II–Ii complexes.

Materials and methods

Mice and cells

I-A^{b}β–GFP knockin (referred to as MHC II–GFP), I-A^{b}β knockout, and Ii knockout mice were previously described (Cosgrove et al., 1991; Bikoff et al., 1993; Boes et al., 2002). The mouse lymphoma cells A20/DNP expressing surface IgM anti-DNP (Watanabe et al., 1988), IIA1.6 (FcγR-defective

variant of A20), and the DO54.8 T cell hybridoma were cultured as reported previously (Lankar et al., 2002). DCs were differentiated from mouse bone marrows cultured during 12 d in a granulocyte/macrophage colony-stimulating factor–containing medium as described previously (Savina et al., 2006).

Antibodies and drugs

The following Abs and inhibitors were used: rat anti–mouse LAMP-1 (BD Biosciences), rabbit anti-Igα (Lankar et al., 2002), rabbit anti-DM (provided by L. Karlsson, Johnson & Johnson Pharmaceutical Research and Development, San Diego, CA), rabbit anti–full-length Ii (JV11; Driessen et al., 1999), rat anti-Ii N terminal (In-1; BD Biosciences), rat anti–I-$A^{b/d}$ (M5114; Bhattacharya et al., 1981), rabbit anti–I-Aβ (Lankar et al., 2002), rabbit anti-Rab5 (provided by J.P. Gorvel, Universite de la Mediterranee Parc Scientifique de Luminy, Marseille, France), goat anti–cathepsin D (Santa Cruz Biotechnology, Inc.), mouse anti-RhoA (provided by P. Chavrier, Centre National de la Recherche Scientifique/Institut Curie, Paris, France), rat anti–α-tubulin (Serotec), rabbit anti-MLC and rabbit antiphospho-MLC (Thr18/Ser19; both were obtained from Cell Signaling Technology), rabbit anti–myosin IIA (Abcam), mouse antiactin (MP Biomedicals), Cychrome-conjugated anti-B220 (BD Biosciences), phycoerythrin-conjugated anti-IgM (BD Biosciences) and phycoerythrin-conjugated anti–I-A^b (BD Biosciences), ML-7 and Y27632 (Calbiochem), blebbistatin (Tocris), and LHVS (provided by H. Ploegh, Whitehead Institute, Cambridge, MA).

Preparation and stimulation of B cells

A single-cell suspension was generated by the mechanical disruption of spleens from 8–12-wk-old mice, and resting mature IgM^+/IgD^+ B cells were purified by negative selection (Miltenyi Biotec). Cell purity was 80–90% as assessed by flow cytometry using anti-IgM, IgD, and B220 Abs. For activation, B cells (10^7 cells/ml for biochemical assay and 5×10^5 B cells for immunofluorescence) were stimulated using multivalent BCR ligands: 10 μg/ml $F(ab')_2$ goat anti–mouse IgM (Cappel) for primary spleen B cells or 10 μg/ml $F(ab')_2$ goat anti–mouse IgG (MP Biomedicals) for IIA1.6 mouse lymphoma cells plus 20 μg/ml $F(ab')_2$ donkey anti–goat (Jackson ImmunoResearch Laboratories). For BCR activation with NP (8-nm diameter; Fe_2O_3; provided by J. Roger, Université Paris 6, Centre National de la Recherche Scientifique, Paris, France), 10 μg/ml $F(ab')_2$ goat anti–mouse IgG or IgM was mixed with 10 μg/ml of recombinant LACK protein and a 3.2 vol of NP.

Immunofluorescence

B cells plated on poly-L-lysine–coated glass coverslips were fixed in 4% PFA for 20 min at RT, and PFA was quenched in PBS plus 1 mM glycine for 10 min. Fixed cells were incubated with Abs in PBS plus 0.2% BSA and 0.05% saponin. For detection of I-A^d–$LACK_{156–173}$ complexes, biotinylated 2C44 and streptavidin-546 (Tyramide Signal Amplification kit; Invitrogen) were used. Immunofluorescence images were acquired on a confocal microscope (LSM Axiovert 720; Carl Zeiss MicroImaging, Inc.) with a 63× 1.4 NA oil immersion objective (Carl Zeiss MicroImaging, Inc.).

Time-lapse analysis

For video microscopy, B cells attached on poly-L-lysine–coated slides were incubated in a Ludin chamber at 37°C in the absence or presence of BCR multivalent ligands. Fluorescence 3D + time images were acquired every 2–5 min during ∼3 h on an inverted fast 4D deconvolution microscope (DMIRB2; Leica) using a PL APO HC 1.4 NA oil immersion objective (Leica). It was equipped with a cooled interline CCD detector (CoolSNAP HQ; Roper) with a pixel size of 6.45 × 6.45 μm, 12 bits of dynamics, and a read-out speed of 20 MHz. Z positioning was accomplished by a piezoelectric driver (10-nm precision and 40-nm repetitiveness; LVDT; Physik Instrument) mounted beneath the objective lens. Illumination was provided by a fast wavelength switcher (DG-4; Sutter Instrument Co.). We used a 2 × 2 binning and a z distance between planes of 0.3 μm, giving a voxel size of 129 × 129 × 300 nm^3, which is compatible with the deconvolution process. Images were deconvolved with the MetaMorph (Universal Imaging Corp.) point-spread function–based iterative constrained modified gold algorithm. Films were reconstructed using MetaMorph 6.2 software.

Immunoelectron microscopy

1–3 × 10^7 of purified spleen B cells not pretreated or pretreated with myosin II inhibitors were stimulated with multivalent BCR ligands (see Preparation and stimulation of B cells section) and processed for immunoelectron microscopy as previously described (Lankar et al., 2002).

Ag presentation assays

OVA was coupled to DNP (Lankar et al., 2002). Monovalent F(ab) anti–mouse IgM was prepared by reducing 4 mg $F(ab')_2$ goat anti–mouse IgM with 1 mg Mesna (Pierce Chemical Co.) and was incubated with 8 mg maleimide-activated OVA (Pierce Chemical Co.). Fractions were purified on a Sephadex 75 column (GE Healthcare) and purity tested by immunoblotting. Spleen B cells from MHC II–GFP mice (I-A^b haplotype) or A20 anti-DNP cells (I-A^d haplotype) not pretreated or pretreated with myosin II inhibitors were used for stimulation of the B097.10 (I-A^b) or DO54.8 T cell hybridomas (I-A^d) as previously described (Lankar et al., 2002).

Immunoprecipitation and pulse-chase analyses

For immunoprecipitations, IIA1.6 cells were not pretreated or pretreated with inhibitors for 1 h at 37°C followed by activation with multivalent BCR ligands. Alternatively, day 12 bone marrow–derived DCs treated with LPS during 30 min were used. Cells were lysed (100 mM Tris, 300 mM NaCl, 0.5% NP-40, and 5% glycerol plus protease cocktail inhibitors), and 900 μg of cell lysates was precleared with rabbit and mouse nonimmune sera and/or protein G–coated Sepharose beads. Ii and MHC class II molecules were immunoprecipitated using the In-1 rat mAb or M5114 rat mAb, respectively. Samples were washed, resuspended in reducing laemmli buffer, boiled, and loaded onto a 12% SDS-PAGE gel. Proteins were transferred to polyvinylidene difluoride membranes (Immobilon-P; Millipore), and membranes were incubated with the appropriate Abs and revealed with ECL (GE Healthcare). Alternatively, gels were directly stained with colloidal Coomassie blue (Bio-Rad Laboratories). Pulse-chase experiments were performed as previously described (Driessen et al., 1999). In brief, spleen B cells (20 × 10^6 cells for each time point) were starved in methionine/cysteine-free RPMI medium for 45 min at 37°C, pulsed with 0.5 mCi [^{35}S]methionine for 30 min at 37°C, further chased for different time points, and lysed, and cell extracts were immunoprecipitated using anti–MHC II Ab.

Endosome purification

50 × 10^6 primary B cells were activated with magnetic NP coupled to anti-BCR Abs for 1 h at 37°C, washed with PBS, and resuspended in cold homogenization buffer (3 mM imidazol, 8% sucrose, 1 mM DTT, 1 mM EDTA, and protease inhibitors). Cells were broken using a cell cracker (Lankar et al., 2002), nuclei and intact cells were removed by centrifugation at 750 *g* for 10 min, and postnuclear supernatants were collected. NP^+ intracellular compartments were semipurified by incubating postnuclear supernatants on a magnet O/N at 4°C. Nonmagnetic and magnetic fractions were recovered. Equal protein quantities of the magnetic fraction were analyzed by SDS-PAGE.

siRNA transfection

4 × 10^5 IIA1.6 cells were electroporated using nucleofactor R T16 (Amaxa) in the presence of 20 nM siRNAs, SMARTpool siRNA, or siGENOME ON-TARGETplus (#1, 5′-GGGCUUAUCUACACCUAUUUU-3′; #2, 5′-AYAAGA-ACCUGCCCAUCUAUU-3′; #3, 5′-GCAGACAAGUACCUCUAUGUU-3′) specific for the *MYH9* gene or negative control duplex siRNA (5′-UUCU-CCGAACGUGUCACGUTT-3′; QIAGEN). Cells were cultured for 96 h at 37°C and analyzed by immunoblotting or immunofluorescence.

Online supplemental material

Videos 1 and 3 show that B cells undergo cell contraction and MHC II–GFP clustering upon BCR stimulation. Video 2 shows the behavior of nonstimulated purified B lymphocytes from MHC II–GFP mice. Videos 4 and 5 show that treatment of BCR-stimulated cells with inhibitors of MLC phosphorylation prevents cell contraction and MHC II–GFP clustering. Fig. S1 A shows that full-length Ii is weakly detected in central lysosome clusters, whereas H2-DM is enriched in these compartments. Fig. S1 B shows that the proteolysis of Ii is induced upon BCR stimulation. Fig. 1 C shows that there is no variation in the steady state levels of MHC class II surface expression at various times after BCR stimulation. Fig. S2 shows that BCR capping is not modified in B cells whose myosin II activity is inhibited. Fig. S3 shows a characterization of the method used to semipurify the endosomes to which BCR–Ag complexes are targeted. Fig. S4 shows that the formation of MHC II–peptide complexes from endogenous proteins is not affected by the inhibitors of myosin II activity. Fig. S5 shows that Ii and MLC colocalize on ER, Golgi, and endosomal membranes. Online supplemental material is available at http://www.jcb.org/cgi/content/full/jcb.200611147/DC1.

We thank Hidde Ploegh for providing MHC II–GFP knockin mice, Michel Bornens for scientific advice, and Sebastian Amigorena, Philippe Benaroch, Federica Benvenuti, Stéphanie Hugues, and Ariel Savina for critical reading of

the manuscript. A.M. Lennon-Duménil specially thanks Pierre Guermonprez for his continuous scientific input, Yohanns Bellaiche for his tremendous help in writing the manuscript, and Guillaume Duménil for constant support.

F. Vascotto and G. Faure-Andre were supported by fellowships from the Fondation pour la Recherche Médicale (FRM) and from the Ministère de la Recherche, respectively. D. Le Roux was supported by a fellowship from the Association pour la Recherche contre le Cancer. P. Vargas and J. Diaz were supported by fellowships from ECOS-CONICYT (project no. C03S01) and from the Universidad Catolica de Chile, respectively. M.I. Yuseff was supported by a postdoctoral fellowship from the Institut Curie and supplemented by the Beca Presidente de la Republica from the Chilean government (Mideplan). This work was supported by funding from the Institut National de la Santé et de la Recherche Médicale, the FRM, and the Institut Curie.

Submitted: 27 November 2006
Accepted: 16 February 2007

References

Aluvihare, V.R., A.A. Khamlichi, G.T. Williams, L. Adorini, and M.S. Neuberger. 1997. Acceleration of intracellular targeting of antigen by the B-cell antigen receptor: importance depends on the nature of the antigen-antibody interaction. *EMBO J.* 16:3553–3562.

Barois, N., F. Forquet, and J. Davoust. 1998. Actin microfilaments control the MHC class II antigen presentation pathway in B cells. *J. Cell Sci.* 111:1791–1800.

Batista, F.D., D. Iber, and M.S. Neuberger. 2001. B cells acquire antigen from target cells after synapse formation. *Nature*. 411:489–494.

Bhattacharya, A., M.E. Dorf, and T.A. Springer. 1981. A shared alloantigenic determinant on Ia antigens encoded by the I-A and I-E subregions: evidence for I region gene duplication. *J. Immunol.* 127:2488–2495.

Bikoff, E.K., L.Y. Huang, V. Episkopou, J. van Meerwijk, R.N. Germain, and E.J. Robertson. 1993. Defective major histocompatibility complex class II assembly, transport, peptide acquisition, and CD4+ T cell selection in mice lacking invariant chain expression. *J. Exp. Med.* 177:1699–1712.

Boes, M., J. Cerny, R. Massol, M. Op den Brouw, T. Kirchhausen, J. Chen, and H.L. Ploegh. 2002. T-cell engagement of dendritic cells rapidly rearranges MHC class II transport. *Nature*. 418:983–988.

Brachet, V., G. Raposo, S. Amigorena, and I. Mellman. 1997. Ii chain controls the transport of major histocompatibility complex class II molecules to and from lysosomes. *J. Cell Biol.* 137:51–65.

Bresnick, A.R. 1999. Molecular mechanisms of nonmuscle myosin-II regulation. *Curr. Opin. Cell Biol.* 11:26–33.

Brown, B.K., and W. Song. 2001. The actin cytoskeleton is required for the trafficking of the B cell antigen receptor to the late endosomes. *Traffic*. 2:414–427.

Byersdorfer, C.A., R.J. Dipaolo, S.J. Petzold, and E.R. Unanue. 2004. Following immunization antigen becomes concentrated in a limited number of APCs including B cells. *J. Immunol.* 173:6627–6634.

Cambier, J.C., C.M. Pleiman, and M.R. Clark. 1994. Signal transduction by the B cell antigen receptor and its coreceptors. *Annu. Rev. Immunol.* 12:457–486.

Carrasco, Y.R., S.J. Fleire, T. Cameron, M.L. Dustin, and F.D. Batista. 2004. LFA-1/ICAM-1 interaction lowers the threshold of B cell activation by facilitating B cell adhesion and synapse formation. *Immunity*. 20:589–599.

Catron, D.M., A.A. Itano, K.A. Pape, D.L. Mueller, and M.K. Jenkins. 2004. Visualizing the first 50 hr of the primary immune response to a soluble antigen. *Immunity*. 21:341–347.

Cheng, P.C., M.L. Dykstra, R.N. Mitchell, and S.K. Pierce. 1999a. A role for lipid rafts in B cell antigen receptor signaling and antigen targeting. *J. Exp. Med.* 190:1549–1560.

Cheng, P.C., C.R. Steele, L. Gu, W. Song, and S.K. Pierce. 1999b. MHC class II antigen processing in B cells: accelerated intracellular targeting of antigens. *J. Immunol.* 162:7171–7180.

Cosgrove, D., D. Gray, A. Dierich, J. Kaufman, M. Lemeur, C. Benoist, and D. Mathis. 1991. Mice lacking MHC class II molecules. *Cell*. 66:1051–1066.

Drake, L., E.M. McGovern-Brindisi, and J.R. Drake. 2006. BCR ubiquitination controls BCR-mediated antigen processing and presentation. *Blood*. 108:4086–4093.

Driessen, C., R.A. Bryant, A.M. Lennon-Dumenil, J.A. Villadangos, P.W. Bryant, G.P. Shi, H.A. Chapman, and H.L. Ploegh. 1999. Cathepsin S controls the trafficking and maturation of MHC class II molecules in dendritic cells. *J. Cell Biol.* 147:775–790.

Fleire, S.J., J.P. Goldman, Y.R. Carrasco, M. Weber, D. Bray, and F.D. Batista. 2006. B cell ligand discrimination through a spreading and contraction response. *Science*. 312:738–741.

Frank, D.J., T. Noguchi, and K.G. Miller. 2004. Myosin VI: a structural role in actin organization important for protein and organelle localization and trafficking. *Curr. Opin. Cell Biol.* 16:189–194.

Gomes, E.R., S. Jani, and G.G. Gundersen. 2005. Nuclear movement regulated by Cdc42, MRCK, myosin, and actin flow establishes MTOC polarization in migrating cells. *Cell*. 121:451–463.

Gupta, N., B. Wollscheid, J.D. Watts, B. Scheer, R. Aebersold, and A.L. DeFranco. 2006. Quantitative proteomic analysis of B cell lipid rafts reveals that ezrin regulates antigen receptor-mediated lipid raft dynamics. *Nat. Immunol.* 7:625–633.

Gupton, S.L., and C.M. Waterman-Storer. 2006. Spatiotemporal feedback between actomyosin and focal-adhesion systems optimizes rapid cell migration. *Cell*. 125:1361–1374.

Hao, S., and A. August. 2005. Actin depolymerization transduces the strength of B-cell receptor stimulation. *Mol. Biol. Cell*. 16:2275–2284.

Jacobelli, J., S.A. Chmura, D.B. Buxton, M.M. Davis, and M.F. Krummel. 2004. A single class II myosin modulates T cell motility and stopping, but not synapse formation. *Nat. Immunol.* 5:531–538.

Kim, Y.M., J.Y. Pan, G.A. Korbel, V. Peperzak, M. Boes, and H.L. Ploegh. 2006. Monovalent ligation of the B cell receptor induces receptor activation but fails to promote antigen presentation. *Proc. Natl. Acad. Sci. USA*. 103:3327–3332.

Kimura, K., M. Ito, M. Amano, K. Chihara, Y. Fukata, M. Nakafuku, B. Yamamori, J. Feng, T. Nakano, K. Okawa, et al. 1996. Regulation of myosin phosphatase by Rho and Rho-associated kinase (Rho-kinase). *Science*. 273:245–248.

Koonce, C.H., and E.K. Bikoff. 2004. Dissecting MHC class II export, B cell maturation, and DM stability defects in invariant chain mutant mice. *J. Immunol.* 173:3271–3280.

Lankar, D., H. Vincent-Schneider, V. Briken, T. Yokozeki, G. Raposo, and C. Bonnerot. 2002. Dynamics of major histocompatibility complex class II compartments during B cell receptor-mediated cell activation. *J. Exp. Med.* 195:461–472.

Lazarski, C.A., F.A. Chaves, and A.J. Sant. 2006. The impact of DM on MHC class II-restricted antigen presentation can be altered by manipulation of MHC-peptide kinetic stability. *J. Exp. Med.* 203:1319–1328.

McHeyzer-Williams, M.G., L.J. McHeyzer-Williams, J. Fanelli Panus, G. Bikah, R.R. Pogue-Caley, D.J. Driver, and M.D. Eisenbraun. 2000. Antigen-specific immunity. Th cell-dependent B cell responses. *Immunol. Res.* 22:223–236.

Mitchison, N.A. 2004. T-cell-B-cell cooperation. *Nat. Rev. Immunol.* 4:308–312.

Nakagawa, T.Y., and A.Y. Rudensky. 1999. The role of lysosomal proteinases in MHC class II-mediated antigen processing and presentation. *Immunol. Rev.* 172:121–129.

Perrin-Cocon, L.A., C.L. Villiers, J. Salamero, F. Gabert, and P.N. Marche. 2004. B cell receptors and complement receptors target the antigen to distinct intracellular compartments. *J. Immunol.* 172:3564–3572.

Peterson, M., and J. Miller. 1990. Invariant chain influences the immunological recognition of MHC class II molecules. *Nature*. 345:172–174.

Pierce, S.K. 2002. Lipid rafts and B-cell activation. *Nat. Rev. Immunol.* 2:96–105.

Poloso, N.J., A. Muntasell, and P.A. Roche. 2004. MHC class II molecules traffic into lipid rafts during intracellular transport. *J. Immunol.* 173:4539–4546.

Qi, H., J.G. Egen, A.Y. Huang, and R.N. Germain. 2006. Extrafollicular activation of lymph node B cells by antigen-bearing dendritic cells. *Science*. 312:1672–1676.

Raiborg, C., T.E. Rusten, and H. Stenmark. 2003. Protein sorting into multivesicular endosomes. *Curr. Opin. Cell Biol.* 15:446–455.

Reth, M., and J. Wienands. 1997. Initiation and processing of signals from the B cell antigen receptor. *Annu. Rev. Immunol.* 15:453–479.

Rosenblatt, J., L.P. Cramer, B. Baum, and K.M. McGee. 2004. Myosin II-dependent cortical movement is required for centrosome separation and positioning during mitotic spindle assembly. *Cell*. 117:361–372.

Savina, A., C. Jancic, S. Hugues, P. Guermonprez, P. Vargas, I.C. Moura, A.M. Lennon-Dumenil, M.C. Seabra, G. Raposo, and S. Amigorena. 2006. NOX2 controls phagosomal pH to regulate antigen processing during crosspresentation by dendritic cells. *Cell*. 126:205–218.

Seabra, M.C., and E. Coudrier. 2004. Rab GTPases and myosin motors in organelle motility. *Traffic*. 5:393–399.

Shin, J.S., M. Ebersold, M. Pypaert, L. Delamarre, A. Hartley, and I. Mellman. 2006. Surface expression of MHC class II in dendritic cells is controlled by regulated ubiquitination. *Nature*. 444:115–118.

Siemasko, K., B.J. Eisfelder, E. Williamson, S. Kabak, and M.R. Clark. 1998. Cutting edge: signals from the B lymphocyte antigen receptor regulate MHC class II containing late endosomes. *J. Immunol.* 160:5203–5208.

Smith, A., M. Bracke, B. Leitinger, J.C. Porter, and N. Hogg. 2003. LFA-1-induced T cell migration on ICAM-1 involves regulation of MLCK-mediated attachment and ROCK-dependent detachment. *J. Cell Sci.* 116:3123–3133.

Straight, A.F., A. Cheung, J. Limouze, I. Chen, N.J. Westwood, J.R. Sellers, and T.J. Mitchison. 2003. Dissecting temporal and spatial control of cytokinesis with a myosin II Inhibitor. *Science*. 299:1743–1747.

Villadangos, J.A., R.A. Bryant, J. Deussing, C. Driessen, A.M. Lennon-Dumenil, R.J. Riese, W. Roth, P. Saftig, G.P. Shi, H.A. Chapman, et al. 1999. Proteases involved in MHC class II antigen presentation. *Immunol. Rev.* 172:109–120.

Watanabe, M., T.H. Watts, J. Gariepy, and N. Hozumi. 1988. Function and behavior of surface immunoglobulin receptors in antigen-specific T cell-B cell interaction. *Cell. Immunol.* 112:226–235.

Watts, C. 2001. Antigen processing in the endocytic compartment. *Curr. Opin. Immunol.* 13:26–31.

Wolf, P.R., and H.L. Ploegh. 1995. How MHC class II molecules acquire peptide cargo: biosynthesis and trafficking through the endocytic pathway. *Annu. Rev. Cell Dev. Biol.* 11:267–306.

Wubbolts, R., M. Fernandez-Borja, I. Jordens, E. Reits, S. Dusseljee, C. Echeverri, R.B. Vallee, and J. Neefjes. 1999. Opposing motor activities of dynein and kinesin determine retention and transport of MHC class II-containing compartments. *J. Cell Sci.* 112:785–795.

Zimmermann, V.S., P. Rovere, J. Trucy, K. Serre, P. Machy, F. Forquet, L. Leserman, and J. Davoust. 1999. Engagement of B cell receptor regulates the invariant chain-dependent MHC class II presentation pathway. *J. Immunol.* 162:2495–2502.